PRTEC-24467

LASER-SCANNING FLUORESCENCE THERMOGRAPHY FOR THERMOFLUID HEAT TRANSFER

Khan Md. Rabbi¹, Jake Carter¹, Juan Sanchez¹, Shawn A. Putnam^{1,*}

¹Mechanical and Aerospace Engineering, University of Central Florida, Orlando, FL 32816 USA

ABSTRACT

Transient heat fluxes in cutting-edge computing systems, electromagnetic switches, and diode-pumped lasers can exceed 50 MW/m², which is nearly the heat flux radiated by the Sun. To manage extreme thermal loads, the State-of-the-Art is to boil and evaporate liquid coolants on micro- and nano-structured heat sinks. This work demonstrates the application of laser-scanning fluorescence thermography to identify the spatiotemporal limits of local, transient hot-spot cooling with impinging pulsed micro-jets and sprays. The laser-scanning fluorescence thermography measurements are based on the fluorescence of PS microspheres and quantum-dot thin-films deposited on FTO-glass heater substrates. The fluorescence-based thermometers are subsequently coated with either Hafnium (Hf) or Titanium (Ti) metal thin-films, serving as both protective coatings and the heater surfaces at near critical heat flux conditions. This work also discusses the fabrication procedure of the fluorescence heater/thermometers with micro-mesh heater surfaces and the corresponding pulsed-jet-boiling data via IR thermography.

KEYWORDS: Pulsed-jet cooling, dip-coating, fluorescence thermography, IR thermography

1. INTRODUCTION

Due to ever-increasing demand for rapid data processing, heat exchanging devices must be capable of combating high thermal loads in transient environments. This problem is also evident in batteries, fuel cells, and many other energy transfer and conversion devices. The intermittent heat loads in such devices introduce many unique challenges – not only from the lack of fundamental understanding but also due to the difficulty in interfacing high heat flux removal techniques in modern devices. Two-phase thermal management techniques – such as spray cooling, pool and flow boiling, and jet impingement cooling – are a class of such cooling methods with both a high heat removal ceiling and unique challenges for interfacing with high energy/power density devices.

Jet impingement cooling has shown to be top performer. This method is especially appealing for its effectiveness in local hot-spot cooling, the high impact velocity of impinging droplets, and a reduced requirement of fluid inventory when compared to other options [1, 2] . Recently, Murshed et al.[3] studied the conjugate heat transfer with jet cooling from a jets of gas-cooled CO_2 . They experimentally observed that maximum cooling effectiveness occurred at film cooling holes. Clark et al.[4] studied heat flux enhancement using two confined jets of HFE7100. They found that the critical heat flux (CHF) was dictated primarily by the jet velocity and the ratio between jet height and diameter (H/d). Lyu et al.[5] studied pulsed jets on semicircular heated surfaces with pulsation frequencies and nozzle-to-surface distance ratios ranging from 0 Hz <f <25 Hz and 1 <H/d <8, respectively. They observed that pulsed jets outperformed steady jets at nozzle-to-surface distance of H/d >6. Huang et al.[6] experimentally measured the effects of pulsed CO_2 jet impingement. It was shown that during pulsed jet, maximum peak of pressure was 33% larger than that of continuous jet.

^{*}Corresponding author: shawn.putnam@ucf.edu

This work investigates the performance of pulsed jet impingement cooling on multi-functional surfaces in the subcooled boiling regime. Structured surfaces with embedded heating and cooling elements can not only be an effective tool for tuning the two-phase cooling performance, but can also be used to characterize the cooling performance in real-time. This investigation introduces the fabrication technique of multi-functional surfaces for combined fluorescence and infrared (IR) thermography and also presents the idea of thermal enhancement during free-stream jet impingement cooling, using the measured temperature and extracted heat transfer coefficient (HTC) maps at different heat flux and jet-pulsation conditions.

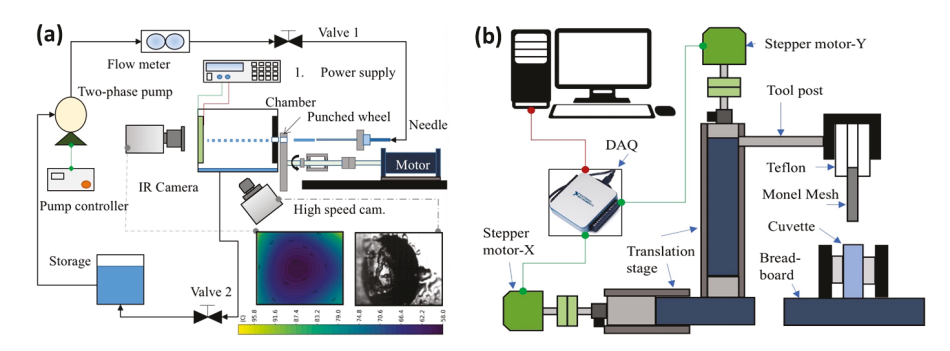


Fig. 1 (a) Schematic diagram of pulsating jet flow loop system. (b) Schematic diagram of dip-coating apparatus for fluorescent particle coatings.

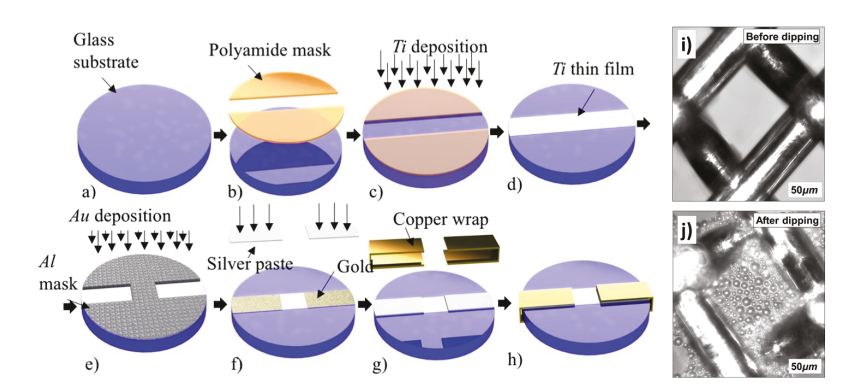


Fig. 2 Heater fabrication: (a) FS substrate, b) polyamide mask application, c) metal (Ti) deposition, d) Ti coated substrate, e) Al mask application and Au deposition, f) Ag-paste application on Au busbars, g) applying Cu wraps, h) final heater. Fluorescent coatings: Ni wire mesh (i) before and (j) after dip-coating.

2. EXPERIMENTAL DETAILS

Fig. 1a shows the pulsed jet cooling apparatus. To generate a continuous flow of water, a custom-built two-phase flow pump developed by RINI technologies is used [7]. The mass flux through the flow loop is measured using K-type flow meter by KI instruments. A stainless-steel syringe needle ($d_0 = 406\mu m$) is used to generate the jets. The spray/jet chamber consists of basic three parts – needle holder, sample holder and chamber housing. The nozzle holder and sample holder can be moved in order to change the relative distance between spray source and heated surface. Fig. 1b shows the computer controlled dip-coating apparatus for fabrication of fluorescent thin-film thermometers.

Fig. 2a illustrates the heater/thermometer fabrication process. Ti or Hf metal thin-film heater/thermometers (typically 50 Ω sheet resistances) were deposited on glass window/substrate by DC magnetron sputtering. For our fluorescence-labeled substrates, the metal coatings were deposited after particle coatings. Figs. 2(i) and 2(j) provides an example of a Ni wire-mesh heater structure before and after particle dip-coating, respectively.

A Mid Wave Infrared (MWIR) thermal camera (FLIR SC7650), 640 x 512 pixels, optical resolution = 100 μ m/pixel) is used to measure the heater surface temperature. Since the glass (fused silica) back is transparent and Ti (or Hf) metal front (boiling surface) is near-opaque in the MWIR region, the thermal camera accurately measures the transient pixel-by-pixel local temperature of the surface. Since, the thin 100nm thick Ti (or Hf) layer is not fully opaque and black thin paint is not fully emissive, the emissivity value (ϵ = 0.9) is adjusted in FLIR ResearchIR MAX software. A Phantom V12.1 camera (optical resolution 44 μ m/pixel) is used either to capture two-phase boiling events or map the temperature evolution of the fluorescent coatings.

For the pulsed-jet boiling experiments the distance between the sample and needle front is kept constant at H=5mm. In our recent work, three different pulsation frequencies were used with Strouhal number (St = $f_p d_{jet}/U_{flow}$) ranging from 0.002 to 0.0045 at a constant Reynolds number (Re = $\rho_w U_{flow}/\mu_w$ = 5450). Heating power is applied from a power supply to generate uniform heat flux through the metal Ti (or Hf) surface heaters. The entire experiment was performed at room temperature conditions (T_{amb} = 20° C and RH = 60%). Since, the MWir camera measures the temperature exactly on Ti (or Hf) boiling surface-layer (due to opaqueness in MWIR region), no 1D conduction model is needed to correct the thermal maps. An in-house Python code handles the three component values, i) pixel-by-pixel temperature value ($T_s(x,y,t)$), ii) local heat flux (q''(x,y,t)) and iii) fluid temperature (T_f). Thus, pixel-by-pixel heat transfer coefficient maps were generated at different heat flux conditions. Gausian filters are employed in Python code to get smoother thermal and heat transfer coefficient maps over the large area (errors within $\pm 2.8\%$).

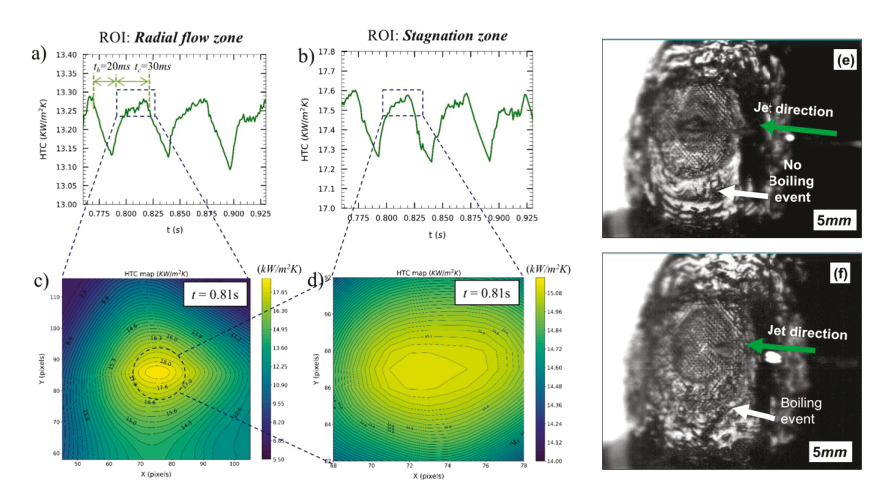


Fig. 3 Temporal HTC profile (a,b) and HTC map (c,d) for heat flux $q'' = 60 \text{ W/cm}^2$, frequency, $f_p = 16.7 \text{ Hz}$, $\dot{m} = 1.56 \text{ gm/s}$, Re = 5490, and St = 0.003. (e,f) High-speed visible images of pulsed-jet boiling on Ni-wire mesh heater/thermometers at input heat fluxes of (e) 10 W/cm² and (f) 60 W/cm².

3. RESULTS AND DISCUSSION

Figs. 3a-d provide data for the temporal changes in the heat transfer coefficient (HTC) profile and average HTC maps at two different regions of interest for pulsation frequency of f_p =16.7 Hz and heat flux 60 W/cm2. As it can be seen, due to pulsation in jet impingement on hot surface, HTC fluctuates uniformly. In jet-ON state or cooling, HTC reaches from 13.12 kW/m2K to 13.3 kW/m2K within 25 ms whereas, during the jet-OFF state or heating state, HTC decreases from 13.3 kW/m2K to 13.12 kW/m2K within 15 ms. During the transitions between the heating and cooling state, HTC maps are analyzed using our IR thermography technique, facilitating pixel-by-pixel understanding of heat transfer enhancement. Figs.3e and 3d provide high-speed camera images for pulsed-jet cooling of the Ni-mesh heater/thermometer. These images show the high speed boiling events during the pulsed-jet impingement on hydrophobic-mesh surfaces at input heat flux of (e) 10 W/cm² (natural convection is dominating) and (f) 60 W/cm² (two-phase cooling dominates) at a Reynolds number of 750. In particular, Fig.3f shows evidence of bubble growth event at a finite radial location from the droplet impacting stagnation zone.

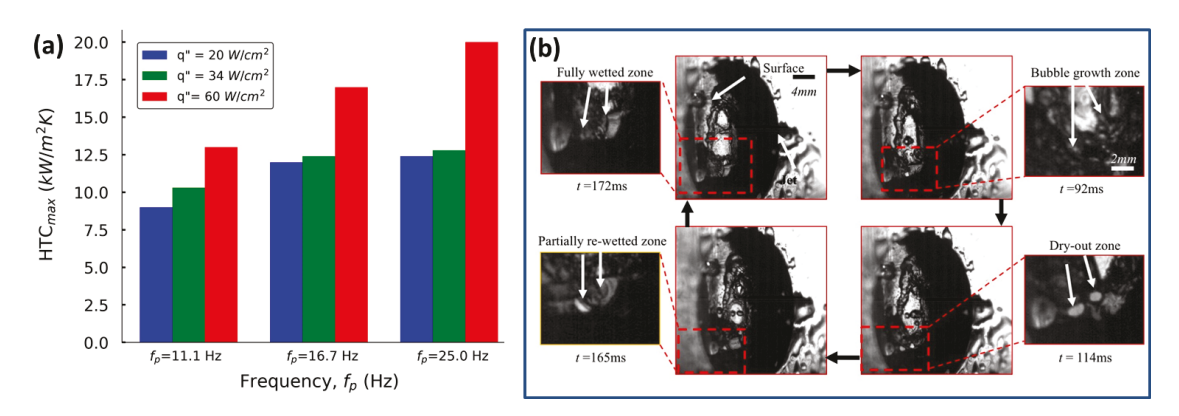


Fig. 4 (a) Heat Transfer coefficients measured in this study at frequencies: $f_p = 11.1$, 16.7, 25.0 Hz and heat fluxes of 20, 34, 60 W/cm². (b) Corresponding high-speed images for pulsed-jet boiling cycles for $f_p = 16.7$ Hz, q'' = 60 W/cm², $\dot{m} = 1.56$ gm/s, and Re = 5490.

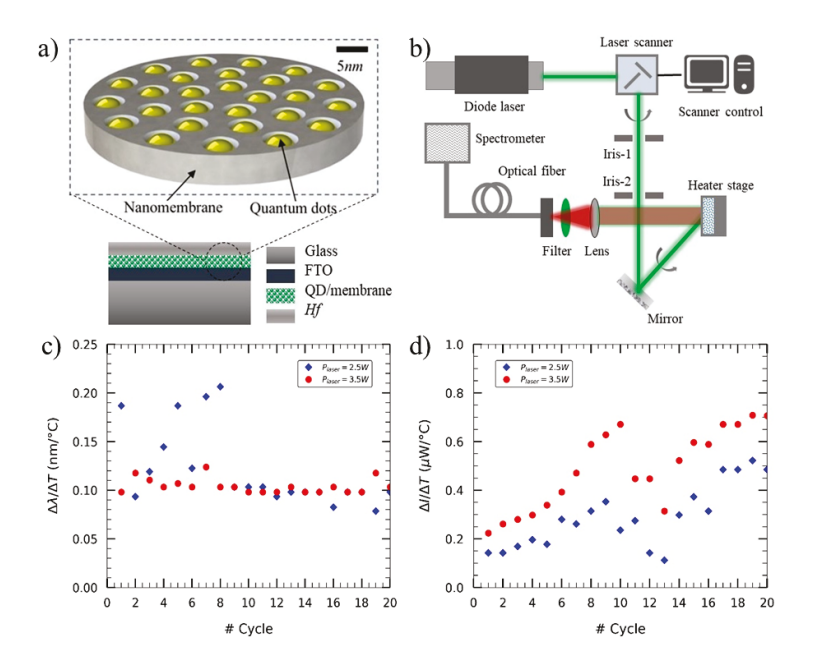


Fig. 5 (a) Al₂O₃ nanomembrane sample embedded with CuInS₂/ZnS Quantum dots (QDs) via dip coating technique (fluorescence peak λ =800 nm, membrane pores: D =20-30 nm. The QD loaded nanomembrane is attached onto Fluorine Tin Oxide (FTO) coated soda lime based glass substrate using Norland Optical Adhesive (NOA). Magnetron sputtering is used to deposit 10 nm of Hf for 1) sustained entrapment of QD into the nanopores and 2) minimized QD oxidation after thermal cycling. (b) Schemmatic of laser-scanning apparatus, where scanning frequencies of f_x =133 Hz and f_y =533 Hz are employed to scan whole Region of Interest (ROI) and to capture T-dependent fluorescence from a uniformly heated QD sample/substrate. Thermal fluorescence coefficients ($\Delta\lambda/\Delta T$ and $\Delta I/\Delta T$) are derived from spectral information from spectrometer. The influence of heating-cooling cycles on thermal fluorescence coefficients are provided in terms of both (c) wavelength shift gradient and (d) intensity shift gradient for two different laser power. For 20 different heating-cooling cycles, uniform thermal fluorescence coefficient of 0.1 nm/C is observed. Spectral intensity gradient regains after relaxation time of 48 hrs. at 10th thermal cycle.

We also note that we observed that maximum heat transfer coefficient is achieved at the center of stagnation zone of jet as suggested by previous illustrations We observe distinct temporal changes in the HTCs for different heat fluxes (20 W/cm², 34 W/cm²) and pulsation frequencies (11.1 Hz and 25 Hz). These results are summarized in Fig. 4a. Fig.4b provides corresponding high-speed camera data of the cyclic boiling events that occur during the pulsed-jet cooling at these moderate heat flux conditions ($\bar{q}'' = 60 \text{ W/cm}^2$). Under steady state conditions,

bubble nucleation is clearly visible at different locations of the surface, especially near the stagnation region. Bubble nucleation occurs at t= 92 ms; moreover, within a few milliseconds of delay the vapor bubbles tend to collapse and near instantly after collapse the dry-out region is generated. The size of dry-out zone increases from t = 93 ms until it reaches maximum in size at t = 114 ms. The fully developed dry-out region coincides with t =165 ms. In this falling film (perturbed by the pulsed jets and also influenced by gravity), asymmetric large wave humps form due to Kaptiza instability. The capillary ripple waves are created from single-peak solution and tends to follow the larger waves after such sudden amplitude increase. Large wave humps are very steady due to these steady capillary ripples. These capillary waves are have longer life since the capillary wave-number is larger than the viscous capillary cut-off.

Figure 5 provides a summary of our success fabricating and testing QD-embedded heater/thermometer samples for combined fluorescence and IR thermometry in transient heat and mass transfer experiments. As the characterization data shows in Figs. 5(c) and 5(d), the approach produces sustainable heat transfer samples/substrates for repeated (or cyclic) heat transfer studies.

4. CONCLUSIONS

MWIR thermography coupled with fluorescence imaging and high-speed visible videography are shown to be a useful techniques to understand and visualize the spatial and temporal evolution of the temperature and flow-field. Both Ti and Hf metals serve as robust heater/thermometers. Dip-coating has shown to be useful for fabricating fluorescent thin-films. With this said, uniform distributions of fluorescent dyes are challenging to fabricate and are needed for accurate mapping of the surface temperature at micron length-scales and sub-millisecond time-scales.

ACKNOWLEDGEMENTS

This material is based on research partially sponsored by the U.S. Office of Naval Research under Grant No. N00014-15-1-2481 and the National Science Foundation under Grant No. 1653396. The views and conclusions contained herein are those of the authors and should not be interpreted as necessarily representing the official policies or endorsements, either expressed or implied, of U.S. Office of Naval Research, the National Science Foundation, or the U.S. Government. The authors also acknowledge financial support for J.S. through UCF's L.E.A.R.N. program.

REFERENCES

- [1] Jambunathan, K., Lai, E., Moss, M. A., and Button, B. L., "A review of heat transfer data for single circular jet impingement." *International journal of heat and fluid flow*, **13**, 106–115 (1992).
- [2] Wolf, D. H., Incropera, F. P., and Viskanta, R., "Jet impingement boiling," In Advances in Heat Transfer, 23, 1–132 (1993).
- [3] Yang, X., Liu, Z., Zhao, Q., Liu, Z., Feng, Z., Guo, F., Ding, L., and Simon, T. W., "Experimental and numerical investigations of overall cooling effectiveness on a vane endwall with jet impingement and film cooling." *Applied Thermal Engineering*, **148**, 1148–1163 (2019).
- [4] Clark, M. D., Weibel, J. A., and Garimella, S. V., *Identification of the Dominant Heat Transfer Mechanisms during Confined Two-phase Jet Impingement*, IEEE (2018).
- [5] Lyu, Y. W., Zhang, J. Z., Liu, X. C., and Shan, Y., "Experimental Investigation of Impinging Heat Transfer of the Pulsed Chevron Jet on a Semicylindrical Concave Plate," *Journal of Heat Transfer*, **141**, 032201 (2019).
- [6] Huang, M., Kang, Y., Wang, X., Hu, Y., Li, D., Cai, C., and Liu, Y., "Experimental investigation on the impingement characteristics of a self-excited oscillation pulsed supercritical carbon dioxide jet," *Experimental Thermal and Fluid Science*, **94**, 304–315 (2018).
- [7] Bostanci, H., He, B., and Chow, L. C., "Spray cooling with ammonium hydroxide," *International Journal of Heat and Mass Transfer*, **107**, 45–52 (2017).